doi.org/10.36721/PJPS.2024.37.4.REG.903-915.1

A novel, non-toxic chitosan modified with lysine to enhance buffer capacity for siRNA delivery

Tianhui Liu[1,3]*, Mei Lin[2,4]*, Chengfei Zhao[1,3] and Aizhu Lin[5,6]

[1]Department of Pharmacy, School of Pharmacy and Medical Technology, Putian University, Putian, China
[2]Department of Medicinal Chemistry, School of Pharmacy, Fujian Medical University, Fuzhou, China
[3]Key Laboratory of Pharmaceutical Analysis and Laboratory Medicine in University of Fujian Province, Putian University, Putian, China
[4]Fujian Key Laboratory of Drug Target Discovery and Structural and Functional Research, Fuzhou, China
[5]Key Laboratory of Technical Evaluation of Fertility Regulation of Non-Human Primates, National Health Commission, Fuzhou, China
[6]Fujian Obstetrics and Gynecology Hospital, Fuzhou, China

Abstract: The present study employed lysine as a modifying agent for chitosan (CS) to synthesise a novel CS derivative (LGCS) intended for siRNA delivery. The successful grafting of lysine to CS was characterized using FT-IR and the introduction of the lysine moiety resulted in improved solubility and buffering capacity of CS. The Zeta potential and size of LGCS/siRNA nanoparticles (NPs) were evaluated using dynamic light scattering (DLS) and the results were verified by transmission electron microscopy (TEM). Evaluation of LGCS's siRNA binding capacity was conducted using a gel retardation assay. The results showed that LGCS could effectively bind to siRNA and form a complex with a hydrated diameter of about 97.2 ± 1.3 nm. Furthermore, cytotoxicity assays conducted on RSC96 cells demonstrated that LGCS exhibited lower toxicity compared to linear polyethyleneimine (PEI) 25k. *In vitro*, cellular uptake assays also revealed that LGCS displayed excellent transfection efficiency. The results of our study lead us to the conclusion that LGCS holds great promise as a gene delivery vector.

Keywords: Cationic polymerization, chitosan, lysine, non-viral vectors, self-assembly.

INTRODUCTION

The development of novel drugs derived from RNA interference (RNAi) technology has led to a significant research focus on small interfering RNA (siRNA) therapeutics (Nastiuk and Krolewski 2016; Setten *et al.*, 2019; Guo *et al*., 2014; Hattab and Bakhtiar, 2020). Although siRNA holds significant potential for cancer treatment, there are still many challenges to be solved before it can be used in clinical application (Karjoo *et al*., 2016; Akhtari *et al*., 2018; Hajiasgharzadeh *et al*., 2018; Rossi and Rossi, 2021). The inefficiency of naked siRNA to accurately deliver to target cells in the face of multiple intracellular inhibitors is the main barrier to clinical siRNA-based therapies (e.g. renal clearance, serum RNA degradation, poor endosomal/lysosomal escape and inefficient cell uptake) (Lee *et al*., 2016; Zhi *et al*., 2016). Therefore, a critical concern for RNA interference-based cancer treatment is the safe and effective delivery of siRNA via appropriate carriers (Yoo *et al*., 2021; Charbe *et al*., 2020).

The utilization of commonly employed viral vectors, including lentiviruses, adenoviruses, retroviruses and adeno-associated viruses (AAVs), in gene therapy has been limited due to their frequent association with cytotoxicity, immunogenicity, broad tropism, carcinogenic potential and restricted DNA packaging capacity (Zhang *et al*., 2012; Pichon *et al*., 2010; Chronopoulou *et al*., 2022). Due to their non-immunogenic qualities and controlled architectures, non-viral vectors are now rapidly becoming more substitutable than viral vectors (Gao *et al*., 2011). A wide range of materials, such as liposomes (Santiwarangkool *et al*., 2019), polymers (Xu *et al*., 2018) and inorganic nanomaterials (Kang *et al*., 2016), have been continuously developed as potential delivery vehicles.

For a considerable duration, extensive research has been conducted on diverse polycations, encompassing both natural and synthetic compounds, as potential non-viral carriers capable of cellular entry and lysosomal evasion. This is attributed to their distinctive property of proton absorption (Shi *et al*., 2017). Because of its remarkable cell penetration, carrying capacity and lysosome escape ability, polyethyleneimine (PEI) has been the most researched material for increased siRNA delivery and is considered the gold standard in transfection (Xue *et al*., 2021; Zhupanyn *et al*., 2020). Although these cationic vectors have a high transfection efficiency, it is crucial to address the challenge of balancing this efficiency with toxicity. Polysaccharides, which are plentiful natural substances, have been extensively studied as polymer carriers because of their biocompatibility and ability to be reconfigured (Altangerel *et al*., 2014; Boisgu´erin *et al*., 2015; Davis *et al*., 2010). The development of effective

**Corresponding authors:* e-mails: liutianhui@ptu.edu.cn

and safe functional carriers using natural polysaccharides to promote the clinical application of RNAi is a rational and significant approach. Among these vectors, chitosan (CS) stands out as an appealing gene delivery vector due to its comparatively low cytotoxicity and elevated positive charge density. The significance of CS to undergo protonation in acidic environments and form complexes with anionic DNA through electrostatic interactions provides strong evidence for its importance in gene delivery (Wang *et al*., 2020; Cao *et al*., 2019, Chuan *et al*., 2019, Bravo-Anaya *et al*., 2019). Although CS exhibits comparable biocompatibility and resistance to DNase degradation as PEI, it demonstrates low transfection efficiency. One contributing factor is the limited rate of endosomal escape associated with CS, primarily attributed to its inadequate buffering capacity that hinders lysosomal escape (Yin *et al*., 2014). To address these limitations, CS derivatives have been synthesised through chemical and biological modifications, resulting in enhanced transfection efficiency for siRNA delivery.

Over time, researchers have gradually explored addressing the challenges of transfection efficiency, toxicity and targeting associated with cationic polymer carriers. Morris and Sharma investigated the synthesis of folic acid and arginine through grafting chitosan, such as ATFP15H. The ATFP15H derivative demonstrated improved nuclear localization and cellular internalization as a result of its superior colloidal stability following conjugation with polyethylene glycol (Morris *et al*., 2010). Sun, Huang and *et al*. introduced a novel CS derivative for siRNA delivery by incorporating poly(histidine-arginine)6(H6R6) peptide into CS. The resulting H6R6-modified CS nanoparticles (NPs) demonstrated superior transfection efficiency and enhanced capacity to escape the endosomes *in vitro* when compared to the unmodified CS NPs (Sun *et al*., 2017). The findings of our recent research indicate that histidine enhances the endosomal escape of siRNAs through its ternary amine (Liu *et al*., 2021). However, we rarely see the use of lysine in gene transfection. We hypothesized that enhancing the transfection efficiency of CS could be achieved through the grafting of lysine onto the CS molecule.

Based on this theory, we introduced lysine into CS to synthesise a novel LGCS polymer for efficient siRNA delivery. *In vitro*, we conducted comprehensive investigations on the particle size, morphology, biocompatibility and transfection efficiency of LGCS/siRNA NPs. Scheme 1 depicts the mechanism of gene silencing.

MATERIALS AND METHODS

Materials

L-lysine, poly (ethylene glycol) (PEG) with a molecular weight (M.W.) of 2000 g·mol^{-1}, hydrochloric acid (HCl), ethanol, acetone and dimethyl sulfoxide (DMSO) are all of analytical purity and were purchased from Sinopharm, China. 1-Ethyl-(3-dimethylaminoprop-yl)carbodiimide hydrochloride (EDC) and CS (with a deacetylation degree of at least 95% and viscosity ranging from 100 to 200 mPa.s) were acquired from Aladdin, China. The dialysis membrane, with a molecular weight cutoff size of 2 kDa, was obtained from Sangon, China. Linear Polyethyleneimine (PEI, M.W. = 25000) was acquired from Alfa Aesar, China. The N-hydroxy succinimide (NHS) compound was acquired from EKEAR. Agarose was purchased from Baygene, China. DAPI solution, Gluta Cell fixative, 50×TAE and 5×RNA Loading Buffer were obtained from Solarbio. The YeaRed Nucleic acid gel stain was purchased from Yeasen, China. The 3-(4, 5-dimethylthiazol-2-yl)-2, 5-diphenyltetrazolium bromide (MTT) reagent was sourced from West Asia, China. DMEM medium, Trypsin Solution, penicillin-streptomycin and RPMI medium were purchased from Hyclone, American. The siRNA and GP-siRNA-Mate plus were obtained from Genepharma, China. Fetal Bovine Serum was purchased from Beit Haemek, Israel. Human cervical carcinoma HeLa cells were procured from the Chinese Academy of Sciences Cell Bank, China. Schwann RSC96 cells and Mouse Melanoma B16F1 cells were sourced from BNCC Cell Bank, China.
siRNA sequence (sense: 5'-UUGUUUUGGAGCGAAAd TdT-3', antisense:5'-UUUCGCUCC-AAAACAAdTdT-3').

Preparation of LGCS polymers

The conjugation of CS and lysine was performed via an amide reaction, utilizing the free primary amino group of CS and the active carboxylic acid group of amino acids, with mediation by EDC/NHS reagents (Abbad *et al*., 2015). The L-lysine was stirred and dissolved in an MES buffer solution (pH = 5.5) at varying concentrations. The carboxyl groups of the lysine were then activated by adding the NHS and EDC in a molar ratio of 1: 1.2: 1.2 (lysine: EDC: NHS) and stirring for 2 hours. Completely dissolved 0.8 g of CS in 40 mL HCl solution (1 %) and mixed with activated amino acid solution, stirred at room temperature for 24 hours. The reacted polymer solution was dialyzed for 72 hours using a dialysis membrane and the deionized water was replaced every 8 hours. Subsequently, the solution was concentrated using a 10% PEG solution (M.W. = 2000g·mol^{-1}). The concentrated solution was then precipitated using twice the volume of acetone and the concentrated polymer was centrifuged at 4000 rpm for 10 minutes. After removal of the supernatant, it was dried in a vacuum drying oven. The lysine to CS feed ratios of 0.2, 1, 2 and 5 are denoted as LGCS0.2, LGCS1, LGCS2 and LGCS5 respectively.

FT-IR analysis

Potassium bromide was used to finely grind the CS and LGCS samples at a ratio of around 1:100. A 330 FT-IR

spectrometer made in America by Thermo Fisher Company was then used to determine the samples' infrared spectra.

Endosomal buffering capacity measurement

According to references, acid-base titration was used to assess the endosomal buffering capacity of PEI 25k, CS, and LGCS throughout a pH range of 3.0 to 11.0, but we made some modifications (Tao *et al*., 2018). In brief, a 25 mL H_2O solution containing 5 mg of polymer was adjusted to pH = 3.0 using an HCl solution (0.1 mol·L^{-1}). Then, each time, 20 µL of a NaOH solution (0.1 mol·L^{-1}) was titrated until pH = 11. A pH meter (PHS-3E, Shanghai Yidian, China) was used to record the pH measurements, and the buffering capacity was compared. Linear PEI 25k, CS and water were employed as control groups.

LGCS/siRNA NPs preparation and characterization

The siRNA was dissolved in DEPC-treated water (0.26 mg·mL^{-1}) and LGCS was dissolved in MES buffer solution pH = 5.5 (1 mg·mL^{-1}). Subsequently, according to the P/R ratio (P: polymer, R: siRNA), the LGCS and siRNA solutions were mixed in equal amounts at different concentrations. The P/R mass ratios of LGCS to siRNA were 0.2, 1, 2, 5 and 10, respectively. Using a Zeta Nano-Sizer (LitesizerTM 500, Anton Paar, Graz, Austria) with a measurement angle of 175 degrees, the size and Zeta potential of LGCS/siRNA NPs were determined (solvent refractive index of 1.333). Samples were drop-cast onto copper wire and air-dried overnight, in preparation for transmission electron microscopy (TEM, Tecnai G20, FEI Company, America) investigation.

Analyzing complex stability

The agarose gel electrophoresis block assay evaluated the stability of the LGCS/siRNA NPs. Each of the samples was loaded onto 1% agarose gels (with 0.01% YeaRed Nucleic acid) in 1 × TAE buffer using a solution of LGCS/siRNA NPs (5 µL, 48 µmol of siRNA) combined with loading buffer (1 mL). The sampled agarose gel blocks were continuously electrophoresed using a horizontal electrophoresis apparatus at a steady voltage of 100 V for 40 minutes. Subsequently, the agarose gels were analyzed at a wavelength of 300 nm using a UV gel image system (Gel Doc TM XR+, BIO-RAD, America).

Cytotoxicity analysis

The cytotoxicity of LGCS was assessed using the MTT assay *in vitro*. RSC96 cells were seeded on a 96-well plate at a density of 5000 cells per well in DMEM complete medium (1% penicillin-streptomycin and 10% FBS) and the cells were incubated for 24 hours at 37°C in a 5% CO_2 incubator. The original culture medium was then aspirated and replaced with a culture medium containing different concentrations of polymers for an additional 24 hours. Then the MTT solution (0.5 mg·mL^{-1}) was added to each well and incubated for 4 hours, 150 µL/well of DMSO was added to dissolve the purple formazan crystal completely. Cell viability was measured at 490 nm using a micro plate reader (1510, Thermo Fisher, America). Cell viability (%) was defined using the following formula (A_{sample} is the absorbance obtained in the presence of polymer and $A_{control}$ is the absorbance of cells that were not treated with polymer):

Cell viability (%) = $(A_{sample}/A_{control}) \times 100\%$ (1)

Cellular uptake of LGCS/siRNA NPs

An amount of 2.5 × 10^4 cells/well B16F1 mouse melanoma cells and HeLa human cervical cancer cells was seeded into 24-well plates and then cultured for 24 hours in a RPMI-1640 complete medium (500 µL/well). The cell medium in each well was then treated with 400 µL fresh medium containing polymer/siRNA complexes (2 µL, containing 19 µmol siRNA) and transfected for 8 hours under standard conditions. Next, the cultured cells were washed twice with PBS solution and fixed with 4% *v/v* glutaraldehyde (400 µL/well) for 20 minutes. Afterward, the cell nuclei were stained with DAPI solution (400 µL, 1 µg·mL^{-1}) for 20 minutes. The cells were washed with PBS solution again and were observed through inverted fluorescence microscopy (LEICA DFC45C, Germany) at 425 nm (blue) and 590 nm (red) filters, GP-siRNA-Mate-Plus ® cationic liposomes were used with an optimal P/R mass ratio of 1 for cellular uptake according to the instructions. Naked siRNA was used as a negative control, while linear PEI 25k was used as a positive control.

The fluorescence intensity of the photographs was analyzed using the fluorescence quantification software Image J. The mean fluorescence intensity (AU) was calculated using the following formula:

Mean fluorescence intensity of CY3 (AU) = Sum of fluorescence intensity of the region/Area of the region. (2)

STATISTICAL ANALYSIS

The statistical analysis was performed with SPSS 20.0. Data were obtained at least in triplicate and expressed as mean + SD (standard deviation). One-way of variance (ANOVA) was used for statistical analysis of the data to compare different groups or the two-tail paired when comparing two groups using the Student's T-test, *$p<0.05$ was considered statistically significant. **$p<0.01$, ***$p<0.001$ and ****$p<0.0001$ are significant differences.

RESULTS

Synthesis and characterization of LGCS polymers

The reaction is illustrated in fig. 1. FT-IR spectroscopy was used to validate the chemical interaction between the CS and lysine (fig. 2). The broad peak at 3400 cm^{-1} in CS

was attributed to the stretching vibration of the hydroxyl bond (O-H). The peak at 1600 cm^{-1} was identified as an amino group ($-NH_2$) bending vibration, and the peak at 1079 cm^{-1} was attributed to stretching vibration of the cyclic-ether bond (C-O-C). The presence of $-CH_2$ groups at the CS and LGCS is responsible for the absorption peak at 2880 cm^{-1}. The successful grafting of lysine on the CS backbone by an amide bond was confirmed by the peaks of N-H bending vibration moving from 1600 cm^{-1} to 1564 cm^{-1} and the C=O stretching vibration due to the amide at 1662 cm^{-1} after coupling with lysine. Because of the poor water solubility of CS, we found that grafting lysine greatly improved the water solubility of CS. Detailed information can be found in the table S1.

Endosomal buffering capacity

Acid-base titration was used to determine the buffering capacity of LGCS derivatives with different degrees of substitution. Unmodified CS, linear PEI 25k, and water were used as a control. It can be seen from fig. 3 that the buffer capacity of LGCS polymers with four different grafting rates has little difference. We calculated the 1/slope from their buffer capacity graphs (table S2). Within the range of pH = 3.0-6.5, the order of $\triangle V_{NaOH}$ change from large to small is LGCS 1 ≈ LGCS 2 > LGCS 5 >LGCS 0.2 >PEI 25k >CS. Therefore, the incorporation of amino acids not only enhances the water solubility of CS but also exerts a significant impact on augmenting the polymer's buffering capacity (Solaro *et al.*, 2010). In contrast to LGCS, which exhibits excellent buffering ability within the pH 3.0-6.5 range, PEI 25k demonstrates an ultra-high buffering capacity spanning from pH 3.0 to 10, potentially contributing to its compromised biocompatibility.

Characterization of LGCS/siRNA NPs

We measured the mean particle sizes and Zeta potentials of LGCS/siRNA with different P/R mass ratios. The values are mean ± SD (n=3). As shown in table S3, the particle size of NPs increases first, then decreases and then increases again with the increase of the P/R mass ratio of the polymer. As shown in tables S3 and S4, except for LGCS5, LGCS complexes can maintain high positive properties and have smaller particle sizes when the P/R mass ratio is 2, and most hydration particle sizes are less than 200 nm. The particle size of LGCS1 is 97.2 ± 1.3 nm when the P/R mass ratio is 2 and less than 100 nm.

The Zeta potential of LGCS/siRNA is negative when the P/R mass ratio for LGCS is 0.2, as depicted in fig. 4. As the P/R mass ratio increases above 1, the NPs exhibit a positive Zeta potential, which further increases with higher P/R ratios. Moreover, all NPs display a Zeta potential above 25 mV when the P/R mass ratio exceeds 5, with some reaching over 30 mV. At a P/R mass ratio of 10, the maximum Zeta potential recorded is 33.3±1.1 mV. These findings suggest that LGCS and siRNA can form positively charged NPs with small particle size, indicating that LGCS/siRNA NPs are likely to be efficiently internalized by cells and exhibit enhanced stability in solution. As illustrated in fig. 4, we observed a significant positive correlation between the Zeta potential of LGCS/siRNA NPs and the P/R mass ratio, with LGCS achieving the minimum particle size at a P/R mass ratio of 2.

The size and morphology of the LGCS/siRNA particles were again confirmed using TEM microscopy (fig. 5). TEM analysis of the LGCS/siRNA formulation revealed elliptical NPs with particle sizes ranging from 100 to 300 nm.

Stability of LGCS/siRNA NPs

Gel electrophoresis block assay was used to evaluate the siRNA binding and protection ability of polymers at different P/R mass ratios. As depicted in fig. 6, the siRNA bands gradually disappeared as the P/R mass ratio of LGCS/siRNA increased. Additionally, when the P/R mass ratio was 0.2 for all LGCS, slight delays in the siRNA bands were observed. The delayed bands observed in LGCS5 at a P/R mass ratio of 10 may be attributed to the instability of LGCS5/siRNA NPs, which can be attributed to their large particle size and low Zeta potential. In contrast, for LGCS0.2 and LGCS1 only a few siRNA bands were observed at a P/R mass ratio of 1, indicating that the LGCS0.2 and LGCS1 polymer is already capable of effectively encapsulating siRNA.

Cytotoxicity of LGCS polymers

The cytotoxicity of LGCS polymers was assessed with an MTT assay using RSC96 cells. fig. 7 shows that LGCS polymers have no significant cytotoxicity for RSC96 cells. At all concentration ratios from 6.25-100 $\mu g \cdot mL^{-1}$, the cell viability of the LGCS polymer was about 90% or more, whereas the cell viability linear PEI 25k was significantly reduced to 15% under the same conditions, and almost all the cells of linear PEI 25k died at 400 $\mu g \cdot mL^{-1}$. fig. 7 demonstrates that the increase in lysine dosage did not result in a significant decrease in cell survival rate. The low polymer concentration exhibited minimal toxicity towards cells, with cell survival rates ranging from 80% to 90%, even when the concentration of LGCS reaches 400 $\mu g \cdot mL^{-1}$. Furthermore, LGCS displayed superior biocompatibility compared to linear PEI 25k based on MTT assay results. In contrast to CS, it appears that lysine-grafted CS has a positive effect on promoting cell growth at lower polymer concentrations.

Based on the above research on the physical and biological properties of four LGCS polymers with different grafting rates, we selected LGCS1 with a P/R mass ratio is 2-1 to siRNA as our main study object for cell uptake. We labeled it as LGCS1 2-1.

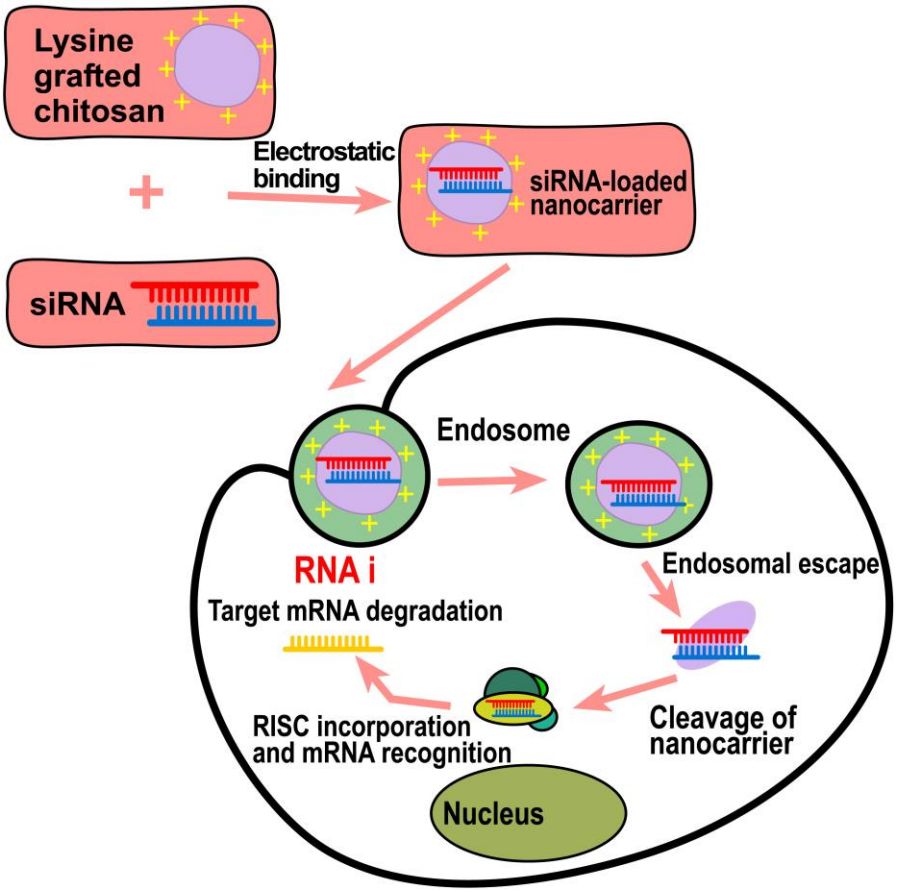

Scheme 1: The process of gene silencing.

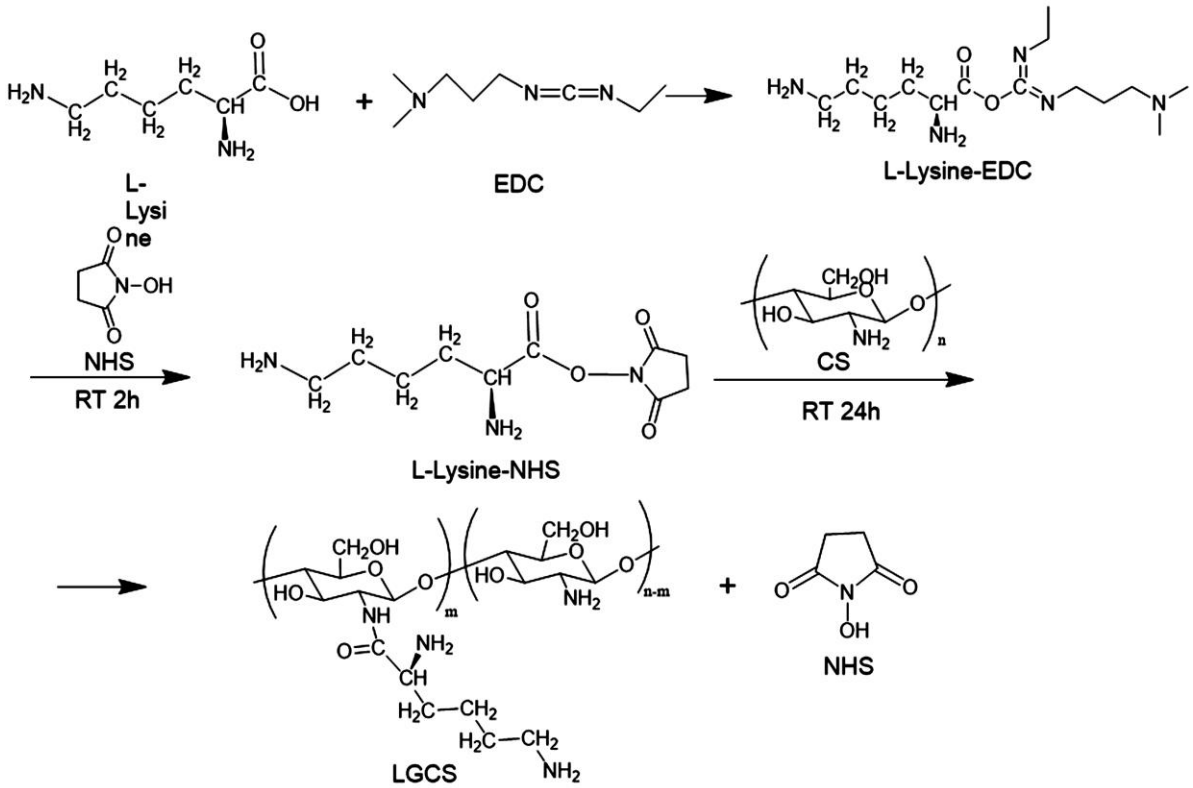

Fig. 1: Reaction schematic of lysine grafted chitosan (LGCS).

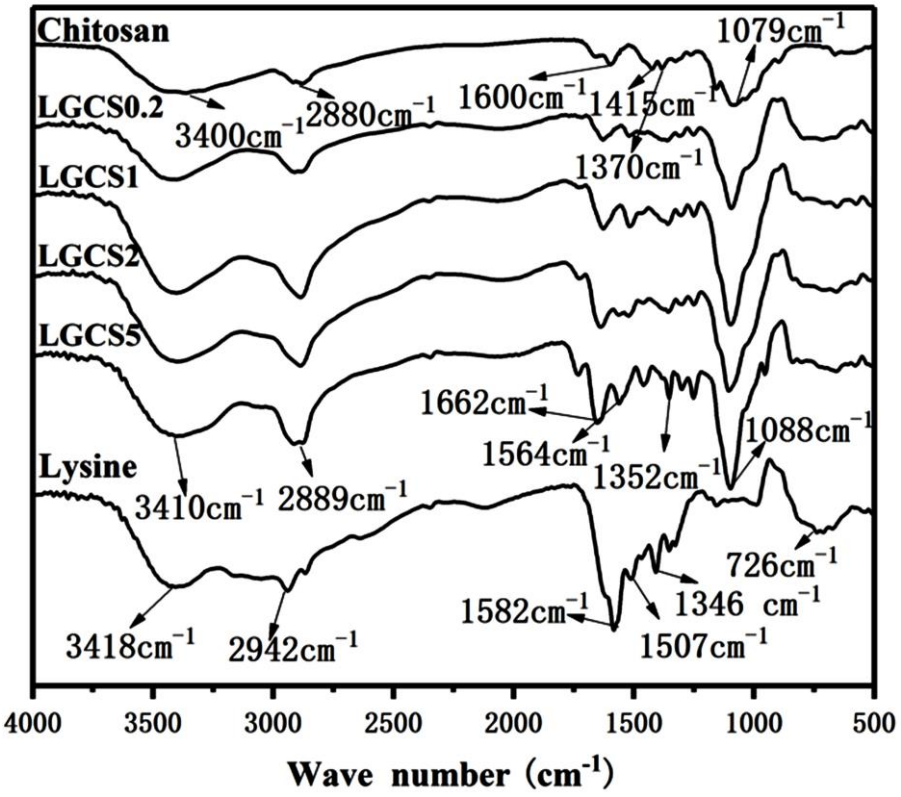

Fig. 2: IR spectra of Chitosan (CS), lysine and LGCS.

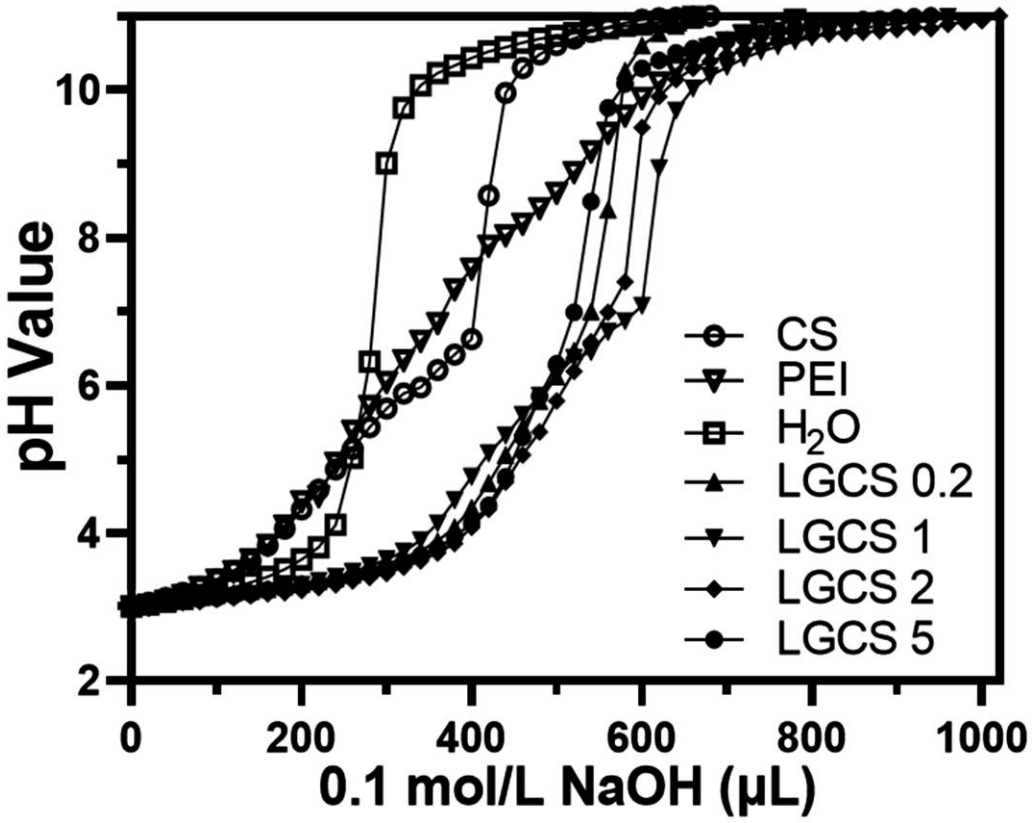

Fig. 3: The acid-base titration curves for water, CS, linear polyethyleneimine (PEI) 25k and LGCS were analysed.

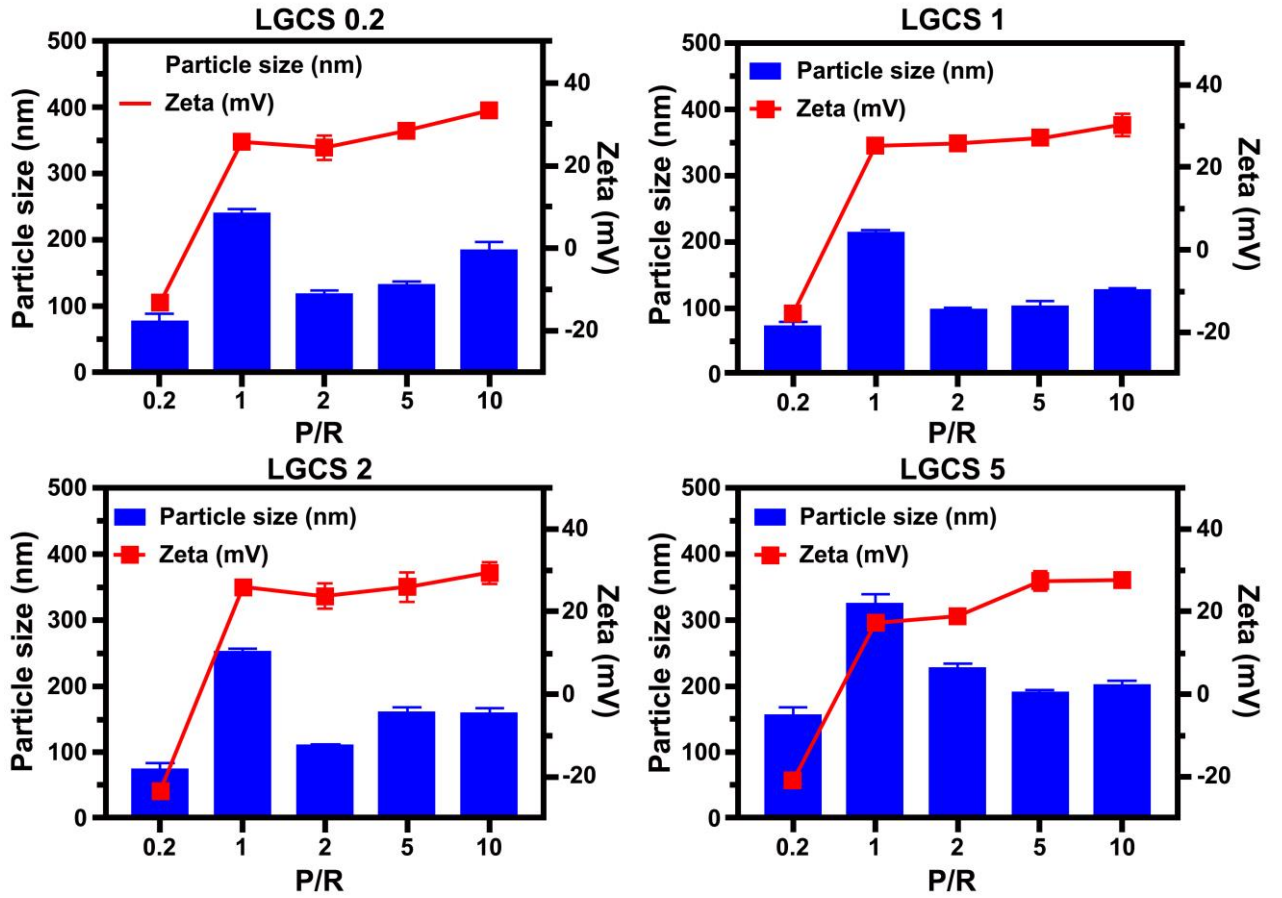

Fig. 4: Relationship between particle size and Zeta potential of LGCS/siRNA NPs.

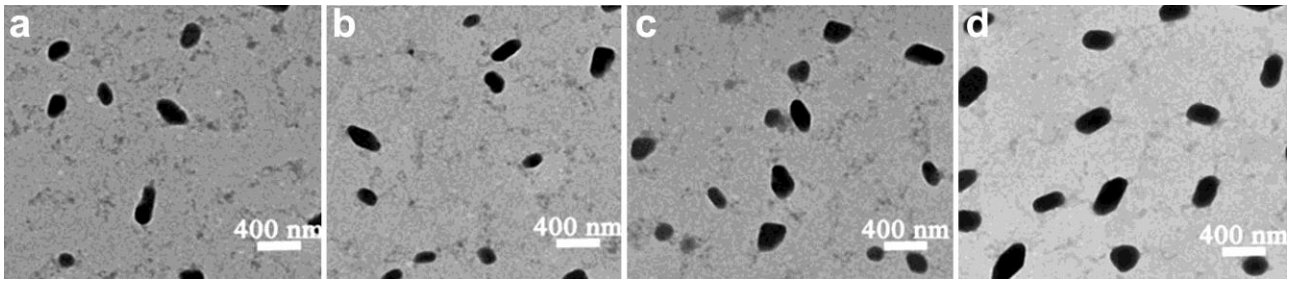

Fig. 5: Transmission electron micrograph of LGCS/siRNA nanoparticles (scale bar = 400 nm). (a) LGCS0.2, (b) LGCS1, (c) LGCS2, (d) LGCS5. All P/R weight ratios are 2, pH=5.5.

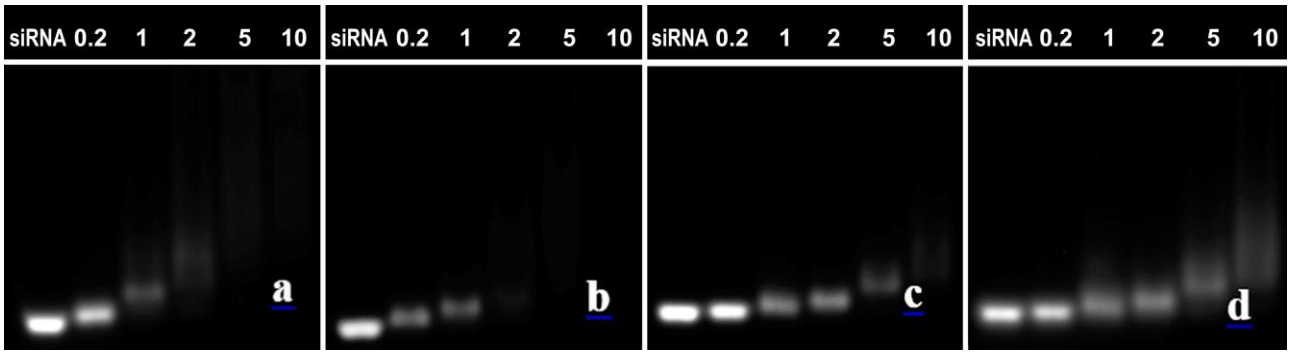

Fig. 6: Agarose gel electrophoresis of LGCS/siRNA NPs with different P/R weight ratios. (a) LGCS0.2, (b) LGCS1, (c) LGCS2 and (d) LGCS5.

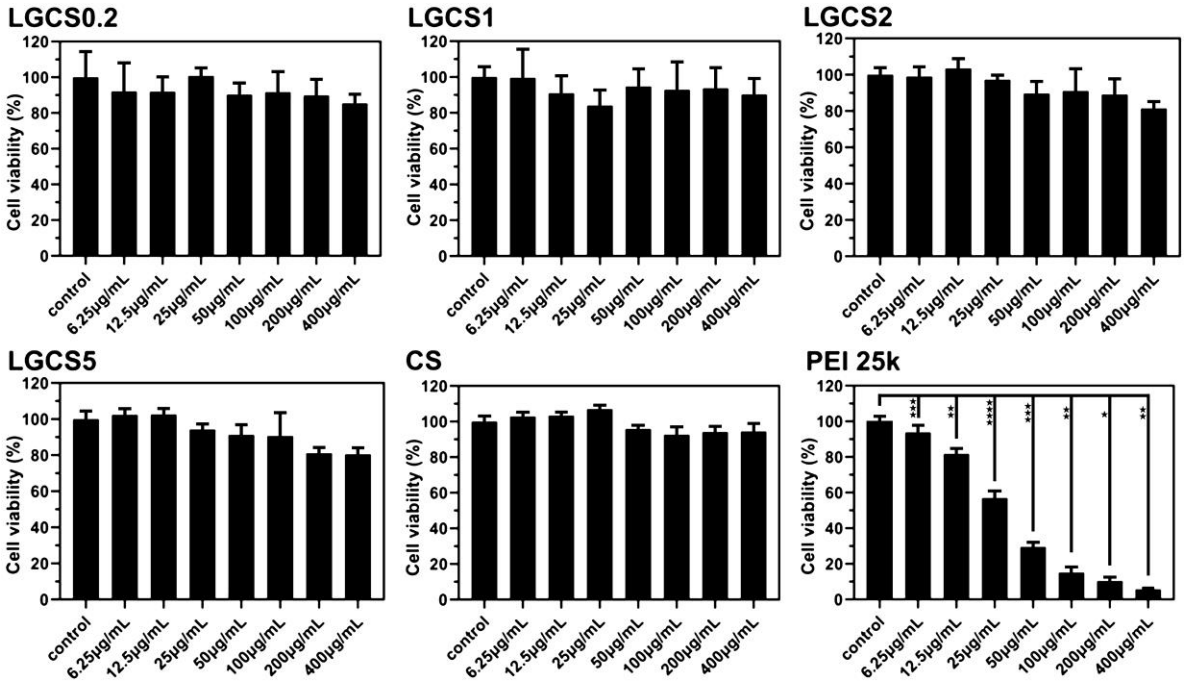

Fig. 7: RSC96 cells viability (%) of polymer (24 h, MTT) at different drug concentrations. Data represent mean ± SD, n = 5, *p<0.05, **p<0.01, ***p<0.001 and ****p<0.0001.

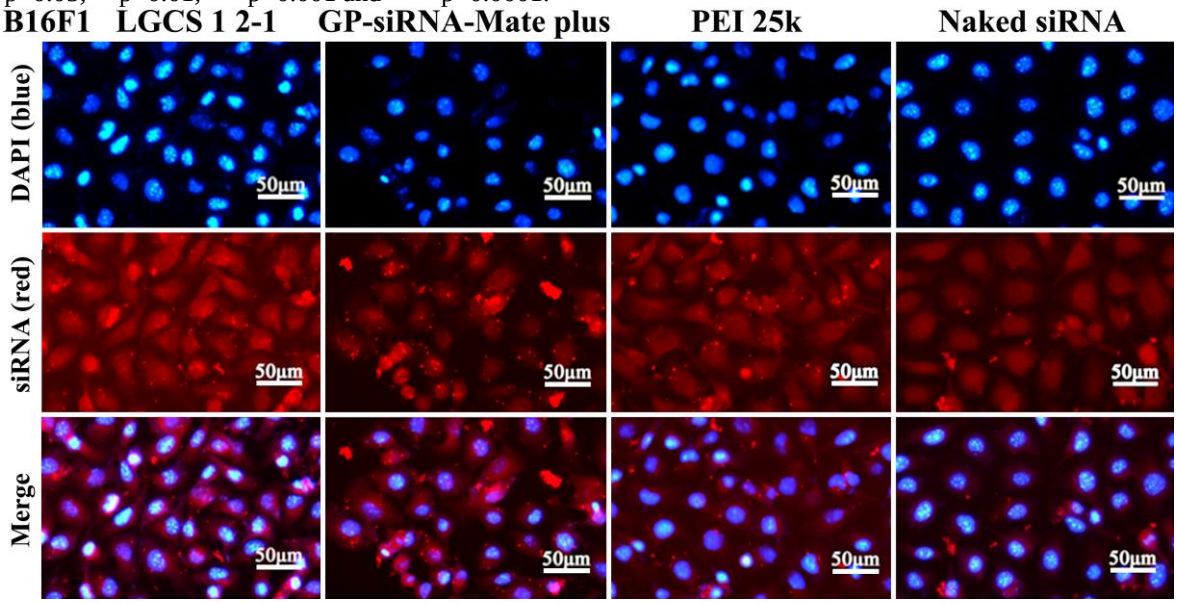

Fig. 8: Typical image of cell uptake siRNA compounds in B16F1 cells (with serum transfection 8 h): Stain the nuclei with DAPI to indicate the position of the nuclei. The combined image shows the nucleus (blue) of B16F1 cells overlapping with siRNA (red).

Cellular uptake of LGCS/siRNA NPs

To assess the *in vitro* cellular uptake of the LGCS derivatives as siRNA vectors, CY3-labeled siRNA was used for the study. As shown in fig. 8, fig. 9 and fig. 10, it is worth mentioning that LGCS1 exhibited enhanced transfection efficiency compared to negative controls such as naked siRNA. In addition, the red fluorescence intensities of LGCS1 in fig. 8 were approach to those of GP-siRNA-Mate plus. As shown in fig. 9, the AU of LGCS1/siRNA in Hela cells was higher than that of commercial liposomes, suggesting that LGCS1 has a suitable gene delivery property. In particular, the AU of LGCS1/siRNA was better than that of PEI 25k, which is also consistent with the results of our buffer capacity experiments. Interestingly, the results also showed that the cellular uptake efficiency of LGCS1 in HeLa cells was stronger than that in B16F1 cells. All these results indicated that LGCS1 was an effective gene delivery system.

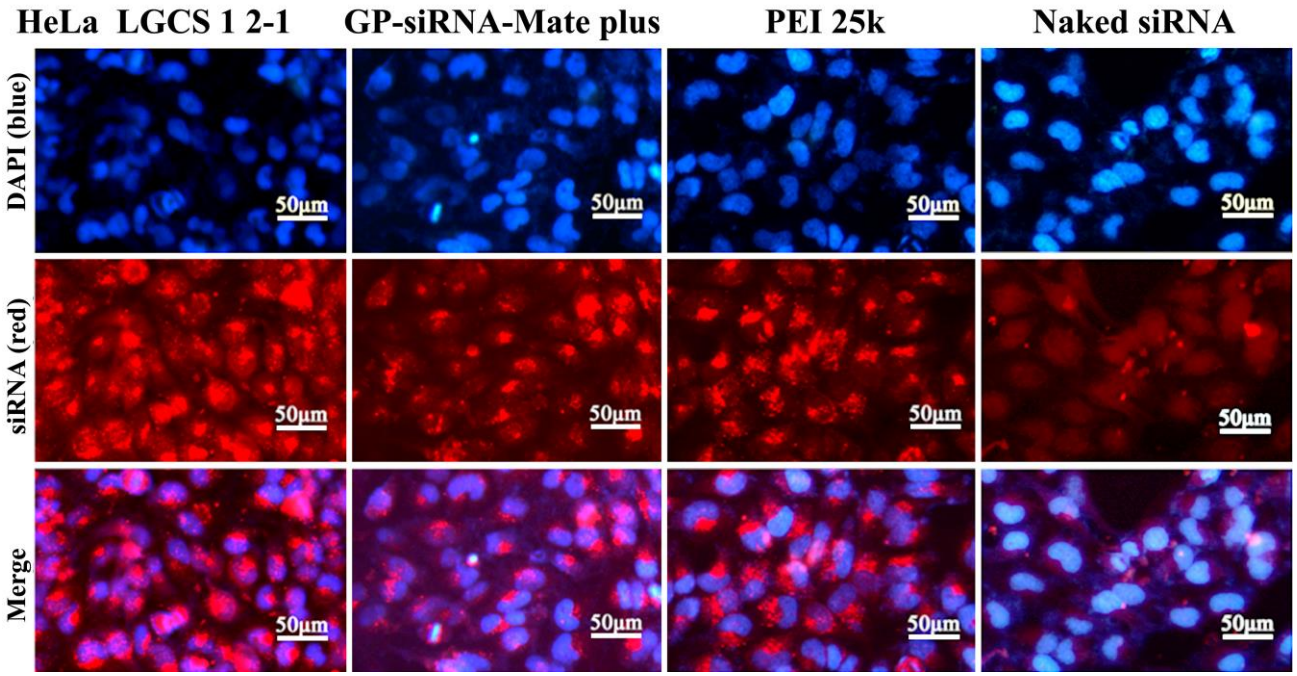

Fig. 9: Typical image of cell uptake siRNA compounds in HeLa cells (with serum transfection 8 h): Stain the nuclei with DAPI to indicate the position of the nuclei. The combined image shows the nucleus (blue) of HeLa cells overlapping with siRNA (red).

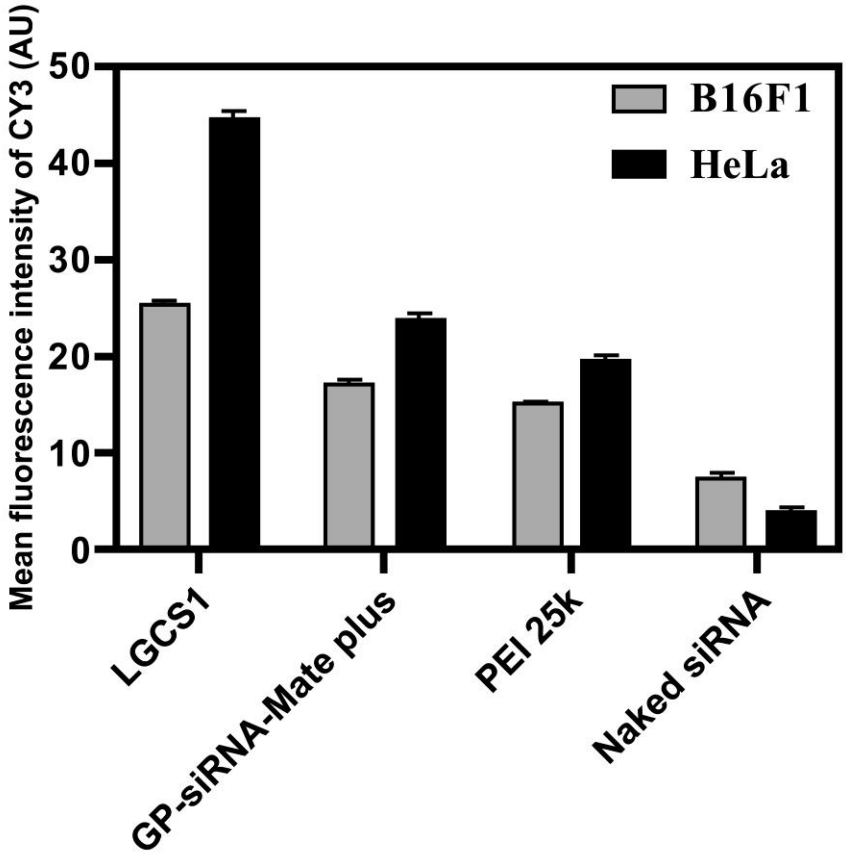

Fig. 10: Mean CY3 fluorescence intensity (AU) of polymer/siRNA in B16F1 and HeLa cells under three different conditions. Data are presented as means ± SD (n = 3).

DISCUSSIONS

To obtain effective gene vectors, amino acids were grafted onto CS via an EDC/NHS-mediated amide reaction to form grafted derivatives of CS. The carboxyl groups of the amino acids were first activated by EDC and then acylated products were generated by reacting NHS with the amino groups at C_2 of CS. The conjugation of lysine and CS was identified by FT-IR spectroscopy. A new peak corresponding to the amide bond of LGCS was observed at 1564 cm^{-1} (fig. 2) (Dumont *et al.*, 2016; Jeong *et al*., 2021).

Further N-acetylation was performed on the sugar-modified CS derivative to increase its water solubility because it has been documented that the degree of N-acetylation determines how crystalline CS becomes, which in turn affects how soluble it is in water. A greater amino ratio enhances the CS-gene complex's stability and encourages stronger cell contact, which boosts transfection efficiency (Desai *et al.*, 2023). The superior water solubility of lysine and the introduction of the amino group on lysine enriched the amino ratio of CS, so the introduction of lysine increased the water solubility of CS. This increased hydrophilicity may promote better dispersion and interaction of LGCS in biological systems, potentially enhancing its performance as a gene delivery vector.

Adequate polymer buffering is essential for endosomal escape and efficient siRNA delivery (Huang *et al.*, 2020). The titration curve of LGCS in fig. 3 showed a slower uptrend and a gentler slope than those of PEI 25k and CS across pH 3.0-6.5, indicating that LGCS has a strong buffering capacity.

Particle size and Zeta-potential are crucial parameters in the design of nucleic acid drug carriers. Particle size can impact the ability to navigate transport barriers in tissues, while Zeta-potential serves as a quantitative measure of charge-induced nanoparticle stability. A Zeta-potential above 25 mV indicates the electrostatic stability of NPs (Sharaf *et al.*, 2020; Guo *et al.*, 2022). In addition to nanoparticle size and surface charge, nanoparticle morphology plays a crucial role in pharmacokinetics and cellular uptake. Therefore, analyzing nanoparticle morphology is essential. All formulations in the study with P/R ratios greater than 1 exhibited positive Zeta potential values ranging from 33.3 ± 1.1 to 17.3 ± 0.8 mV (table S4). The LGCS1 2-1 formulation was selected as the siRNA carrier system due to its small particle size (97.2 ± 1.3 nm) and high Zeta potential (25.8 ± 1.7 mV).

According to agarose gel electrophoresis, the Zeta potential and particle size of LGCS/siRNA complexes are correlated with their stability. We used agarose gel electrophoresis to measure the degree of complex binding to siRNA because naked siRNA will show distinct bands if the complex does not fully encapsulate it. The physical stability of complexes during the electrophoretic correlates with the amount of positive charge on the surface of NPs (Miele *et al.*, 2021). The appearance of siRNA bands indicates a decrease in the stability of its binding to the NPs, indicating weak interaction between LGCS2, LGCS5 and siRNA via ionic adsorption. Consequently, the siRNA was released in the presence of an electric field. These findings are consistent with previous studies of Zeta potential, which suggest that the ability of siRNA to bind to carriers is influenced by the positive charge on the surface of the NPs.

CS is biodegradable, minimizing side effects on cells. LGCS biosafety and siRNA delivery into B16F1 and HeLa cells were further investigated. As fig. 8 and fig. 9 show, in the B16F1 and HeLa cells incubated with LGCS1/siRNA, a large number of red fluorescence was observed. The fluorescence intensity analyzed by Image J (fig. 10) of the LGCS1/siRNA group was stronger than that of the GP-siRNA-Mate plus/siRNA group and PEI 25k/siRNA group, indicating that LGCS1 could effectively deliver siRNA with better ability than commercial liposome. To improve cellular uptake of CS, amino acids with positively charged R groups were preferred (Luo *et al.*, 2023). Lysine's positively charged R group enhances the positive charge of CS. LGCS demonstrated comparable ability to GP-siRNA-Mate plus in siRNA delivery due to the lysine modification that enhanced the buffering capacity of the CS. The successful delivery of siRNA by LGCS1 may also be attributed to properties of NPs, which have smaller sizes and larger specific surface areas than non-nanomaterials, thus increasing the ability of siRNA to cross the cell membrane. Given the low toxicity of LGCS polymers to RSC96 cells and the high efficiency of siRNA delivery, it could be valuable as a transfection reagent or as a potential material for siRNA delivery.

CONCLUSION

LGCS polymers were prepared by linking lysine and CS to overcome their low cellular uptake efficiency and poor endosomal escape capacity for siRNA delivery. The resulting LGCS polymer was thoroughly characterized both physicochemically and biologically to demonstrate its efficacy as a gene delivery vector. FT-IR analysis confirmed the successful conjugation of -C=O and -N-H groups, while acid-base titration revealed that the buffering capacity of the LGCS derivative surpassed that of PEI 25k and CS within the pH range of 3.0-6.5. The utilization of DLS measurements and TEM micrographs demonstrated the effective condensation of siRNA and formation of elliptical nanostructured particles with a positive charge, which were smaller than 200 nm in size. The polymer exhibited a protective effect on siRNA,

preventing degradation by RNase. Furthermore, the incorporation of lysine was found to enhance both the internalization efficiency and buffering capacity of CS molecules. *In vitro* cell experiments revealed that non-toxic LGCS NPs could rapidly evade cellular uptake barriers. Compared to the polymer PEI 25k, the LGCS1 showed a better transfection efficiency in both B16F1 and HeLa cell lines, even in the presence of 10% serum. The enhanced transfection efficiency can be attributed to the buffering capacity provided by lysine residues. These findings substantiate the potential application of LGCS polymers as siRNA transfection agents. The investigation and analysis of additional mechanisms and factors contributing to the enhancement of buffer capacity by lysine grafted polymer are warranted for further scholarly examination and discourse.

ACKNOWLEDGMENTS

This work was supported by the [Science and Technology Project of Education Department of Fujian Province (CN) #1] under Grant [number: JAT200522]; [Natural Science Foundation of Fujian Province (CN) #2] under Grant [number: 2020J01633]; [Scientific Research Project of Putian University (CN) #3] under Grant [number: 2022059]; [National Natural Science Foun-dation (CN) #4] under Grant [number: 81703477]. A preprint has previously been published in Research Square under the following link https://www.researchgate.net/publication/34963-9824.

REFERENCES

Setten RL, Rossi JJ and Han S (2019). The current state and future directions of RNAi-based therapeutics. *Nat. Rev. Drug Discov*., **18**(6): 421-446.

Guo J, Cahill MR, McKenna SL and O'Driscoll CM (2014). Biomimetic nanoparticles for siRNA delivery in the treatment of leukaemia. *Biotechnol. Adv*., **32**(8): 1396-1409.

Hattab D and Bakhtiar A (2020). Bioengineered siRNA-based nanoplatforms targeting molecular signaling pathways for the treatment of triple negative breast cancer: Preclinical and clinical advancements. *Pharmaceutics*, **12**(10): 929.

Nastiuk KL and Krolewski JJ (2016). Opportunities and challenges in combination gene cancer therapy. *Adv. Drug. Deliver. Rev*., **98**: 35-40.

Karjoo Z, Chen XG and Hatefi A (2016). Progress and problems with the use of suicide genes for targeted cancer therapy. *Adv. Drug. Deliv. Rev*., **99**(Pt A): 113-128.

Akhtari J, Tafazoli A, Mehrad-Majd H and Mahrooz A (2018). Nanovehicle-based Small Interfering RNA (siRNA) Delivery for therapeutic purposes: A new molecular approach in pharmacogenomics. *Curr. Clin. Pharmacol.*, **13**(3): 173-182.

Hajiasgharzadeh K, Somi MH, Shanehbandi D, Mokhtarzadeh A and Baradaran B (2018). Small interfering RNA-mediated gene suppression as a therapeutic intervention in hepatocellular carcinoma. *J. Cell. Physiol.*, **234**(4): 3263-3276.

Rossi JJ and Rossi DJ (2021). siRNA drugs: Here to stay. *Mol. Ther*., **29**(2): 431-432.

Lee SJ, Kim MJ, Kwon IC and Roberts TM (2016). Delivery strategies and potential targets for siRNA in major cancer types. *Adv. Drug. Deliver. Rev.*, **104**: 2-15.

Zhi D, Zhao Y, Cui S, Chen H and Zhang S (2016). Conjugates of small target-ing molecules to non-viral vectors for the mediation of siRNA. *Acta. Biomater*., **36**(1): 21-41.

Yoo JY, Yeh M, Kaur B and Lee TJ (2021). Targeted delivery of small noncoding RNA for glioblastoma. *Cancer Lett*., **500**: 274-280.

Charbe NB, Amnerkar ND, Ramesh B, Tambuwala MM, Bakshi HA, Aljabali AAA, Khadse SC, Satheeshkumar R, Satija S, Metha M, Chellappan DK, Shrivastava G, Gupta G, Negi P, Dua K and Zacconin FC (2020). Small interfering RNA for cancer treatment: Overcoming hurdles in delivery. *Acta Pharm. Sin. B*, **10**(11): 2075-2109.

Zhang SB, Zhao YN, Zhi DF and Zhang SF (2012). Non-viral vectors for the mediation of RNAi. *Bioorg. Chem.*, **40**: 10-18.

Pichon C, Billiet L and Midoux P (2010). Chemical vectors for gene delivery: Uptake and intracellular trafficking. *Curr. Opin. Biotech.*, **21**(5): 640-645.

Chronopoulou L, Falasca F, Di Fonzo F, Turriziani O and Palocci C (2022). siRNA transfection mediated by chitosan microparticles for the treatment of HIV-1 infection of human cell lines. *Materials*, **15**(15): 5340.

Gao Y, Liu XL and Li XR (2011). Research progress on siRNA delivery with nonviral carriers. *Int. J. Nanomedicine*, **6**: 1017-1025.

Santiwarangkool S, Akita H, Khalil IA, Abd Elwakil MM, Sato Y, Kusumoto K and Harashima H (2019). A study of the endocytosis mechanism and transendothelial activity of lung-targeted GALA-modified liposomes. *J. Control. Release*, **307**: 55-63.

Xu X, Wu J, Liu S, Saw PE, Wei T, Li Y, Krygsman L, Yegnasubramanian S, Marzo AMD and Shi J (2018). Redox-responsive nanoparticle-mediated systemic RNAi for effective cancer therapy. *Small*, **14**(41): 1802565.

Kang J, Joo J, Kwon EJ, Skalak M, Hussain S, She Z, Ruoslahti GE, Bhatia SN and Sailor MJ (2016). Self-sealing porous silicon-calcium silicate core-shell nanoparticles for targeted siRNA delivery to the injured brain. *Adv. Mater.*, **28**(36): 7962-7969.

Shi B, Zheng M, Tao W, Chung R, Jin D, Ghaffari D and Farokhzad OC (2017). Challenges in DNA delivery and recent advances in multifunctional polymeric DNA

delivery systems. *Biomacromolecules*, **18**(8): 2231-2246.

Xue L, Yan YF, Kos P and Chen XP (2021). PEI fluorination reduces toxicity and promotes liver-targeted siRNA delivery. *Drug Deliv. Transl. Re.*, **11**: 255-260.

Zhupanyn P, Ewe A, Buch T, Malek A, Rademacher P, Muller C, Reinert A, Jaimes Y and Aigner A (2020). Extracellular vesicle (ECV)-modified polyethylenimine (PEI) complexes for enhanced siRNA delivery *in vitro* and *in vivo*. *J. Control. Release*, **319**: 63-76.

Altangerel A, Cai J, Liu LX, Wu YG, Baigude H and Han JF (2016). PEGylation of 6-amino-6-deoxy-curdlan for efficient *in vivo* siRNA delivery. *Carbohyd. Polym*., **141**: 92-98.

Boisgu´erin P, Deshayes S, Gait MJ, O'Donovan L, Godfrey C, Betts CA, Wood MJA and Lebleu B (2015). Delivery of therapeutic oligonucleotides with cell penetrating peptides. *Adv. Drug Deliver. Rev.*, **87**: 52-67.

Davis ME, Zuckerman JE, Choi CH, Seligson D, Tolcher A, Alabi CA, Yen Y, Heide JD and Ribas A (2010). Evidence of RNAi in humans from systemically administered siRNA via targeted nanoparticles. *Nature*, **464**(7291): 1067-1070.

Wang W, Xue C and Mao X (2020). Chitosan: Structural modification, biological activity and application. *Int. J. Biol. Macromol*., **164**: 4532-4546.

Cao Y, Tan YF, Wong YS, Liew MWJ and Venkatraman S (2019). Recent advances in chitosan-based carriers for gene delivery. *Marine. Drugs*, **17**(6): pp. 381.

Chuan D, Jin T, Fan R, Zhou L and Guo G (2019). Chitosan for gene delivery: Methods for improvement and applications. *Adv. Colloid Interface Sci*., **268**: 25-38.

Bravo-Anaya LM, Fernandez-Solis KG, Rosselgong J, Nano-Rodriguez JLE, Carvajal F and Rinaudo M (2019). Chitosan-DNA polyelectrolyte complex: Influence of chitosan characteristics and mechanism of complex formation. *Int. J. Biol. Macromol.*, **126**: 1037-1049.

Yin H, Kanasty RL, Eltoukhy AA, Vegas AJ, Dorkin JR and Anderson DG (2014). Non-viral vectors for gene-based therapy. *Nat. Rev. Genet.*, **15**(8): 541-555.

Morris VB and Sharma CP (2010). Folate mediated *in vitro* targeting of depolymerised trimethylated chitosan having arginine functionality. *J. Colloid. Interf. Sci.*, **348**(2): 360-368.

Sun P, Huang W, Kang L, Jin MJ, Fan B, Jin HY, Wang QM and Gao ZG (2017). siRNA-loaded poly(histidine-arginine)6-modified chitosan nanoparticle with enhanced cell-penetrating and endosomal escape capacities for suppressing breast tumor metastasis. *Int. J. Nanomed*., **12**: 3221-3234.

Liu TH, Lin M, Wu F, Lin AL, Luo DS and Zhang ZY (2021). Development of a nontoxic and efficient gene delivery vector based on histidine grafted chitosan. *Int. J. Polym. Mater. Po*., **71**(10): 717-727.

Abbad S, Zhang Z, Waddad AY, Munyendo WL and Zhou J (2015). Chitosan-modified cationic amino acid nanoparticles as a novel oral delivery system for insulin. *J. Biomed. Nanotechnol*., **11**(3): 486-499.

Tao L, Chen S, Zhang S, Wu X, Wu P, Miao B and Cai X (2018). Transferrin-functionalized chitosan-graft-poly (l-lysine) dendrons as a high-efficiency gene delivery carrier for nasopharyngeal carcinoma therapy. *J. Mater. Chem. B*., **6**(26): 4314-4325.

Solaro R, Chiellini F and Battisti A (2010). Targeted delivery of protein drugs by nanocarriers. *Materials*, **3**(3): 1928-1980.

Dumont VC, Mansur HS, Mansur AAP, Carvalho SM, Capanema NSV and Barrioni BR (2016). Glycol chitosan/nanohydroxyapatite biocomposites for potential bone tissue engineering and regenerative medicine. *Int. J. Biol. Macromol*., **93**: 1465-1478.

Jeong EJ, Lee J, Kim HS and Lee KY (2021). In vitro cellular uptake and transfection of oligoarginine-conjugated glycol chitosan/siRNA nanoparticles. *Polymers*, **13**(23): 4219.

Desai N, Rana D, Salave S, Gupta R, Patel P, Karunakaran B, Sharma A, Giri J, Benival D and Kommineni N (2023). Chitosan: A potential biopolymer in drug delivery and biomedical applications. *Pharmaceutics*, **15**(4): 1313.

Huang G, Chen Q, Wu W, Wang J, Chu PK, Bai H and Tang G (2020). Reconstructed chitosan with alkylamine for enhanced gene delivery by promoting endosomal escape. *Carbohydr. Polym*., **227**: 115339.

Sharaf OZ, Taylor RA and Abu-Nada E (2020). On the colloidal and chemical stability of solar nanofluids: From nanoscale interactions to recent advances. *Phys. Rep*., **867**: 1-84.

Guo L, Shi DD, Shang MM, Sun X, Meng D, Liu XX, Zhou XY and Li J (2022). Utilizing RNA nanotechnology to construct negatively charged and ultrasound-responsive nanodroplets for targeted delivery of siRNA. *Drug Delivery*, **29**(1): 316-327.

Miele D, Xia X, Catenacci L, Sorrenti M, Rossi S, Sandri G, Ferrari F, Rossi JJ and Bonferoni MC (2021). Chitosan oleate coated PLGA nanoparticles as siRNA drug delivery system. *Pharmaceutics*, **13**(10): 1716.

Luo JX, Chen JF, Liu Y, He YJ and Dong WJ (2023). A novel form of arginine-chitosan as nanoparticles efficient for siRNA delivery into mouse leukemia Cells. *Int. J. Mol. Sci.*, **24**(2): 1040

Table S1: Solubility of CS and LGCS polymers in different pH solutions

Group	pH value of the solution						
	2	3	4	5	6	7	8
CS	+	+	-	-	-	-	-
LGCS0.2	+	+	+	+	+	+	+
LGCS1	+	+	+	+	+	+	+
LGCS2	+	+	+	+	+	+	+
LGCS5	+	+	+	+	+	+	+

Note: "+" means soluble, "-" means insoluble, and "±" means partially soluble

Table S2: The 1/Slope of acid-base titration curves for water, CS, linear polyethyleneimine (PEI) 25k, and LGCS.

Group	Equation	Slope	1/Slope
CS	y=0.0147x+1.8463	0.0147	68.0
H_2O	y=0.0158x+2.2396	0.0158	63.3
PEI 25k	y=0.0118x+2.4663	0.0118	84.7
LGCS0.2	y=0.0129x+0.9772	0.0129	77.5
LGCS1	y=0.0106x+1.4064	0.0106	94.3
LGCS2	y=0.0107x+1.3259	0.0107	93.5
LGCS5	y=0.0116x+1.3259	0.0116	86.2

Table S3: Particle size of LGCS/siRNA complexes with different P/R weight ratios. Data are presented as mean ± SD (n = 3).

Wight ratio P/R	LGCS0.2 (nm)	LGCS1 (nm)	LGCS2 (nm)	LGCS5 (nm)
0.2	78.0 ± 11.1	72.2 ± 6.3	75.2 ± 8.1	157.0 ± 11.1
1	239.4 ± 6.9	213.8 ± 2.7	252.7 ± 4.1	325.5 ± 12.4
2	120.6 ± 1.9	97.2 ± 1.3	110.7 ± 0.7	227.3 ± 5.3
5	133.2 ± 3.7	103.5 ± 6.1	161.0 ± 6.5	190.5 ± 0.9
10	184.6 ± 12.5	127.0 ± 0.8	159.3 ± 7.4	203.1 ± 4.3

Table S4: Zeta potentials of LGCS/siRNA complexes with different P/R weight ratios. Data are presented as mean ± SD (n = 3).

Wight ratio P/R	LGCS0.2(mV)	LGCS1(mV)	LGCS2(mV)	LGCS5(mV)
0.2	-13.4 ± 1.4	-15.5 ± 1.6	-23.3 ± 4.7	-20.7 ± 0.9
1	25.8 ± 0.7	25.2 ± 0.2	25.9 ± 1.5	17.3 ± 0.8
2	24.3 ± 2.9	25.8 ± 1.7	23.9 ± 2.9	19.0 ± 0.5
5	28.5 ± 1.4	27.0 ± 1.4	26.0 ± 3.4	27.4 ± 2.1
10	33.3 ± 1.1	30.3 ± 2.5	29.5 ± 2.3	27.7 ± 1.0